Science, Engineering and Social Science Series
ISSN/e-ISSN: 2541 – 0369/2613 – 988X
DOI: 10.51971/joma.v7n1.1301002023
Vol. 7, No. 1, 2023, Printed in the Indonesia

Identification of Aquifer, Ground Water-Bearing Rock, using Vertical Electrical Sounding (VES): East Lampung Case Study

Intan Andriani Putri [1,*], Risky Martin Antosia[1], Alhada Farduwin[1], Reza Rizki[1], Yudha Styawan[1], Sillak Hasiany[2]

[1]*Geophysical Engineering Study Program, Sumatera Institute of Technology*
[1]*Environmental Engineering Study Program, Sumatera Institute of Technology*

A one-dimensional geo-electrical method using Vertical Electrical Sounding (VES) has been carried out to model lithology and identify an aquifer, a water-bearing rock, in East Lampung to provide the water needs of the poultry breeding industry (PT. X) that is going to be established in the near future. Two VES points had been surveyed using Schlumberger electrode configuration to achieve good depth penetration and good vertical resolution. Geophysical modeling is not unique, overcoming this issue could be done using a global inversion method. A global inversion technique called Particle Swarm Optimization (PSO) was performed to create more reliable subsurface lithology, resulting in around 5 – 11% errors. The PSO algorithm deployed here took 1.000 particle numbers with ω=0.8; α_l=1.8; and α_g=2. The result shows that the study area's lithology consists of Tuff, Sandy Tuffaceous, and Shaley Tuff. Sandy Tuffaceous is identified as a confining aquifer zone. There are two potential aquifer zones, Aquifer I and Aquifer II. Aquifer II has more potential as water resources of the industry due to its thickness, moreover, it is topped by impermeable Shaley tuff that prevents local climate effects such as rain that could decrease water quality.

Keywords: Aquifer, Vertical Electrical Sounding (VES), Schlumberger configuration, Particle Swarm Optimization (PSO)

1. INTRODUCTION

The Indonesian poultry industry is a key player in the nation's economy, making a considerable contribution by providing 65% of the total animal protein supply and employing around 10% of the national workforce. Over the past few decades, the production methods have undergone considerable evolution and modernization.

Water stands as the paramount nutrient when considering the holistic health and performance of commercial poultry. It is assumed that a five-pound broiler is estimated to consume approximately 18 pounds of water, surpassing the roughly 10 pounds of feed it consumes. Maintaining an adequate water supply is of utmost importance to ensure that a sufficient quantity of water is readily available to meet the needs. A company in East Lampung (PT. X) is starting a new chicken breeding farm and is attempting to meet its needs for - water from the groundwater. Groundwater is usually contained in a rock layer called an aquifer. A geophysical method called Vertical Electrical Sounding (VES) that deploys electric current injected into the sub-surface is a powerful tool to identify aquifers. It measures the potential and then calculates its apparent resistivity (called observed apparent resistivity) [1-4]. A subsurface resistivity model is built and used to calculate a synthetic apparent resistivity. The synthetic and observed apparent resistivity were then compared to calculate its error. Once the error is minimal, the resistivity model that is used to create the synthetic apparent resistivity is accepted as a subsurface resistivity representation. Due to the resistivity value, the lithology could be determined, thus the aquifer could be identified based on the lithology. Therefore, this research was conducted to model lithology as the recommendation for aquifer identification to fulfill the water supply of PT. X.

[*]*Email Address: andriani.putri@tg.itera.ac.id*

This research aims to build a lithology model so the aquifer characteristics: lithology, type, depth, and thickness, can be identified.

2. BACKGROUND THEORY

A. *Regional Geology*

Geographically, Sumatra Island is located in an archipelagic region between the Indo-Australian plate and the Asian plate, resulting in a variety of natural landscape features such as trenches, volcanic arcs, fore-arc basins, and back-arc basins. This region is located in the Lampung Province, with coordinates of 103°30'-106°50' E longitude and 3°00'-6°00' S latitude.

Mangga et al. interpret the Bandar Lampung area as composed of several rock formations that formed during different time spans. The Gunung Kasih Formation (Pzg) consists of altered rocks from the Paleozoic era and serves as the bedrock. Subsequently, non-conformably overlying volcanic rocks form the Tarahan Formation (Tpot) from the Paleocene era, which is intruded by granite and granodiorite formations from the early Miocene era. The youngest rocks are the Lampung Formation (QTI) and Young Volcanic Formation (Qhv), from the Pliocene and Pleistocene epochs. The survey location falls within the Lampung Formation, which comprises volcanic tuffs, rhyolitic tuffs, welded tuffs, tuffaceous mudstone, and tuffaceous sandstone (see Figure 1).

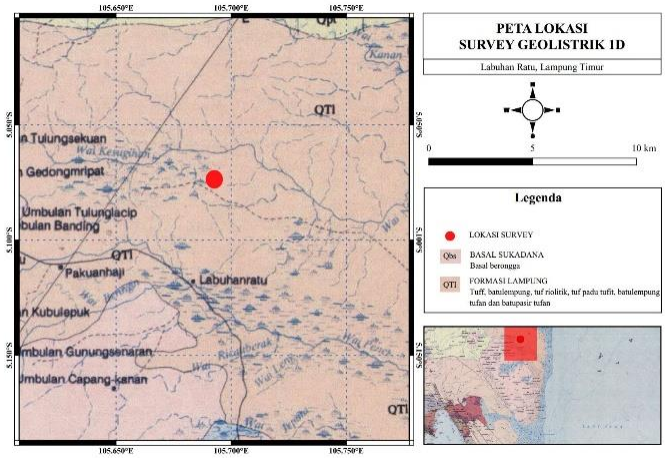

Figure 1. Regional geology map of the study area

B. *Vertical Electrical Sounding*

Electric flows inside the earth, where the earth is considered a homogeneous isotropic media so that the electric flows in all directions. As a result of the air's extremely high level of resistance, the current can only extend below the earth's surface, where it forms a half-ball equipotential field. In general, the type of earth resistances is not homogeneous, meaning that the calculated are apparent resistivity (ρ_a) [4]. The apparent type of resistance does not directly indicate the resistance of the medium but reflects the distribution of medium-type resistivity values. This is because the earth is a non-homogeneous medium consisting of numerous layers with different types of resistances, affecting the electrical potential measured. The apparent type of resistance is denoted by ρ and so that this equation can be written as in:

$$\rho_a = K\frac{\Delta V}{I} \tag{1}$$

where, K is the geometrical factor that depends on the setting of the four electrodes or the lock configuration [2]. The research employs the Schlumberger configuration, which is characterized by a relatively deep current penetration, approximately 1/5th of the distance between the current electrodes. This configuration is favored for depth sounding over the Wenner array due to its streamlined field procedure, simplicity, and the availability of master curves and software for result analysis, as noted by Ekwe et al. [6]. The Schlumberger configuration offers several advantages compared to other configurations, including superior depth penetration when compared to the Wenner configuration and enhanced vertical accuracy compared to the dipole-dipole configuration, as mentioned by Reynolds. The Schlumberger array represents a modification of the gradient array, where the potential electrodes are positioned at the center of the array, while the spacing of the current electrodes is adjusted, as highlighted by Pratt [8]. Figure 2 shows an electrode installation scheme in the Schlumberger configuration. Schlumberger configuration uses 4 electrodes with 2 current electrodes (AB) and 2 potential electrodes (MN) [5-10] arranged in a single line. The distance of each electrode in figure 2 as follows:

$$r_1 = r_4 = (L - l) \tag{2}$$
$$r_2 = r_3 = (L + l) \tag{3}$$

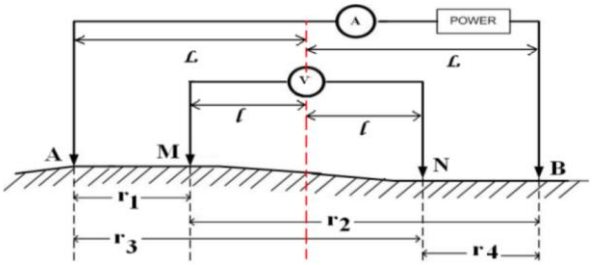

Figure. 2. Electrode position of Schlumberger Configuration

With $L = \frac{AB}{2}$ and $l = \frac{MN}{2}$. Configuration factor for Schlumberger configuration is given as follows.

$$K = \frac{\pi(L^2 - l^2)}{2l} \tag{4}$$

finally, apparent resistivity could be calculated using:

$$\rho_a = \frac{\pi(L^2 - l^2)}{2l}\frac{\Delta V}{I} \tag{5}$$

The disparity in the constituent factors and compositions of rocks results in the uncertainty and variability of subsurface resistivity values. This phenomenon is evident in Table 1 below:

Table I. Resistivity of some rock [1]

Lithology	Resistivity (Ωm)
pyrite	$5x10^2$ - $8 x10^4$
quartz	$5x10^2$ - $8x10^5$
rock salt	$3x10^1$ - $1x10^{13}$
granite	$2x10^2$ - $1x10^4$
andesit	$1.7x10^2$ - $45x10^4$
basalt	$2x10^2$ -$1x10^5$
Limestones	$5x10^2$ -$1x10^4$
sandstones	$2x10^2$ -$8x10^3$
shales	$2x10^1$ -$2x10^3$
sand	$1x10^0$ - $1x10^3$
clay	$1x10^0$ - $1x10^2$
ground water	$5x10^{-1}$ -$3x10^2$
sea water	$2x10^{-1}$
dry gravel	$6x10^2$ -$1x10^4$
Lava	$1x10^2$ -$1x10^4$
alluvium	$1x10^1$ -$8x10^2$
gravel	$1x10^2$ -$6x10^2$

C. Inverse Modeling

Field measurements yield data pertaining to subsurface conditions and properties, with the recorded outcomes constituting observational data. The status and properties of the rock are then connected with this observational data to extract information through mathematical modelling. The information thus acquired, in the form of parameters derived from the mathematical model, is referred to as inverse modelling [11].

Grandis [12] wrote that the inversion process should exhibit a good correlation between the model response and the observed data, typically represented by an objective function that needs to be minimized. Inversion modelling can only be performed when the relationship between data and model parameters or the function derived from forward modelling is known. To obtain the best solution (optimum), it is necessary to optimize the objective function [12].

Non-linear inversion with a linear approach is widely used in geophysical inverse modelling such as Newton – Raphson method, Levenberg Marquardt, etc. Those methods could provide a good correlation but the main issue was the probability of being trapped in local minima is high. Hence, there is a need to search for the optimal solution on a global scale in order to attain the global minimum.

The inversion method that can be employed to obtain a global minimum value is Particle Swarm Optimization (PSO). The Particle Swarm Optimization (PSO) algorithm is designed based on the social behaviour of individual particles on a surface, akin to the swarming of bees and herds of zebras in locating a target. Within the population, each swarm (particle) moves randomly and has unique information. Particles that move towards and discover the target first will be followed by other particles in pursuit of the same target [13].

The particles that reach the target initially provide information concerning the distance (position) and the achieved velocity. Velocity and position are represented as vectors with vector V (velocity) and vector X (position) [14]. When conducting inversion on the objective function of the Vertical Electrical Sounding (VES) curve, the estimated model parameters (m) are obtained from vector X, which consists of layer thickness (h) and true resistivity (ρ). The application of PSO in inversion can be carried out through the following steps:

a) To determine the size of the search space, both the number of particles and iterations must be taken into account.
b) Initial positions are generated by randomly populating the initial population (X) where:
X : $X_1^0, X_2^0, X_3^0, \dots, X_j^i$;

i = iteration;
j = n-th particle;
n = Total number
V values are assumed to be zero for all particles ($V_1^0 = V_2^0 = \dots = V_i^0 = 0$)

c) Estimations are made for the objective function values $f[X_1^0]; f[X_2^0]; f[X_3^0]; \dots; f[X_j^0]$.

d) Estimates for parameters l and g are also made. Parameter l represents the best position (X) of a particle in reaching the target during the iterations, and parameter g represents the best velocity (V) of a particle across the entire population during the iterations while minimizing the value of f.
e) Updates to the velocity (V) and position (X) of each particle are performed during each iteration using the PSO algorithm.

The values of velocity (V) and position (X) for each particle can be obtained using the following equations [15]:

$$V_i^{k+1} = \omega V_i^k + \phi_1.(g^k - X_i^k) + \phi_2.(l_i^k - X_i^k) \quad (4)$$

$$X_i^{k+1} = X_i^k + V_i^{k+1} \quad (5)$$

With:
$\phi_1 = r_1 a_g, \phi_2 = r_2 a_l, r_1, r_2$
$l_i(k)$ = Best position of particle-i
$g(k)$ = Global best position.
ω = Inertia weight
ϕ_1, ϕ_2 = Global and local accelerations.
a_l, a_g = Local's and global acceleration's constants.

e regression is discretized using RR-PSO using the following equations to produce velocity and acceleration in the time domain

$$V(t+\Delta t) = \frac{V(t)+\phi_1\Delta t(g(t)-X(t))+\phi_2\Delta t(l(t)-X(t))}{1+(1-\omega)\Delta t+\phi\Delta t^2} \quad (6)$$

$$X(t+\Delta t) = X(t) + V(t+\Delta t)\Delta t \quad (7)$$

With $\phi = \phi_1+\phi_2$ *and* $\Delta t = 1$

Determining the best parameters in PSO inversion, such as ω, a_l, and a_g, is crucial for achieving optimal results. This can be done through parameter tuning, as indicated by previous research [15,16], with values set at ω = 0.8, a_l = 1.8, and a_g = 2. In the study of aquifer identification using VES data [16], the best optimization results were obtained by determining the number of particles and the parameters used. The resulting model is evaluated based on the error percentage and the Similarity Index (SI). The Similarity Index (SI) is used to quantify the similarity between the inverted model solution and the actual data. SI values range from 0% to 100%, with higher values indicating a better match between the inverted model solution and the actual model. SI can be calculated using the following equation [16].

$$SI = \left(1 - \frac{\sum_m^M \frac{|P_m^{inv}-P_{ml}^r|}{P_m^r}}{M}\right) x\ 100\% \quad (8)$$

Where:

P_m^{inv} : Model parameter obtained from inversion

P_m^r : Real model parameter

M : Model

3. METHODOLOGY

Two points of One Dimension VES data were measured in 2023 using the Naniura geo-electricity apparatus. Schlumberger Electrode configuration was chosen. The line length for each point is written in Table III. The PBG_1 point has the shortest length due to the field condition that did not support the wire stretch. With these lengths, it was expected to model the lithology up to 40 m accurately.

Table II. Length of each line

Lines	Length (m)
PBG_1	160
PBG_2	210

In VES curve modelling using Particle Swarm Optimization (PSO) inversion, calculations are performed to search for the best-fitting model, as indicated by a converging error curve. Convergence is marked by the absence of further modification in subsequent iterations, indicating that the constructed model has reached its - optimum state, resulting in the smallest possible error. The PSO inversion is executed with the following parameters (see Table III).

Table III. PSO parameter

Parameters	Value
Particle number	1.000
ω	0.8
α_l	1.8
α_g	2.0

4. RESULT AND DISCUSION

Each data point exhibits a varying number of iterations required to achieve convergence. Error curves for data points PBG_1 and PBG_2 are depicted in Figure 3. For data point PBG_1, convergence is reached after 9 iterations resulting error of around 5%. On the other hand, for PBG_2, it takes 16 iterations to attain a minimum error below 11.05%.

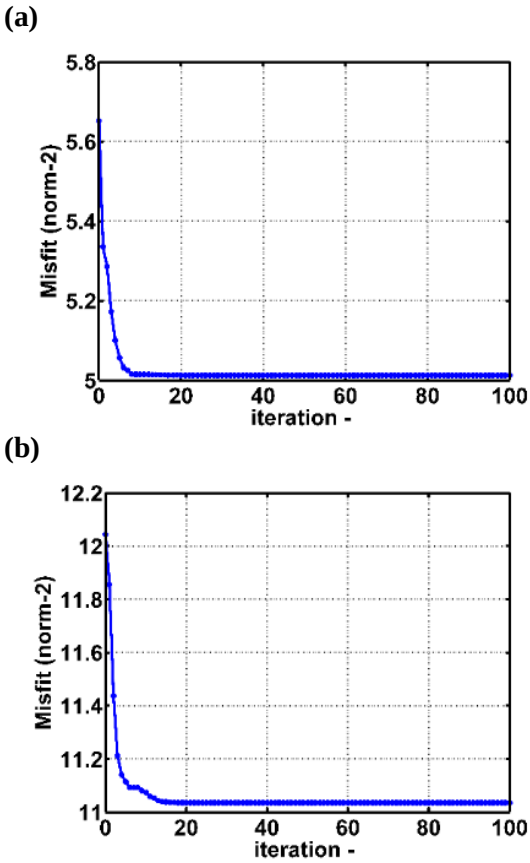

Figure 3. Error curve for (a) PBG_1 and (b) PBG_2

The fitting of the PSO inversion curve and the resistivity model at each depth for data points PBG_1 and PBG_2 is illustrated in Figure 3. Blue dots represent the observed data and red lines represent the calculated data. The graph shows how well components fit together. The use of PSO

in VES data gave a better result as the method minimizes the probabilistic of trapped in local minimum.

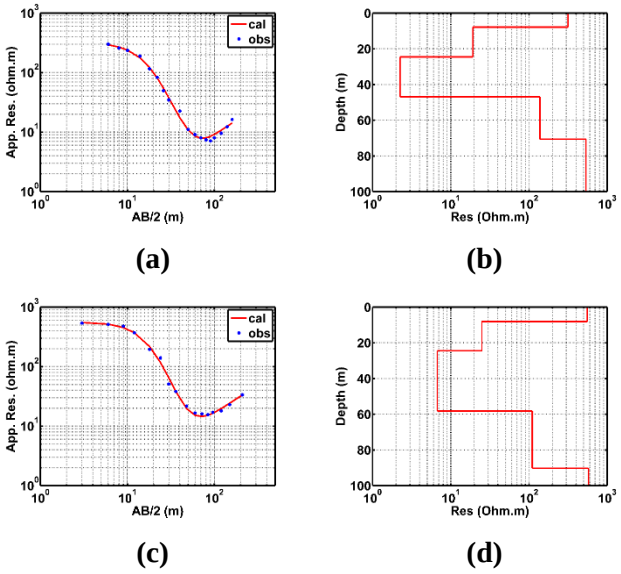

Figure 4. Fitting of the PSO inversion curve for PBG_1 (a) and PBG_2 (c), along with the resistivity model at various depths for PBG_1 (c) and PBG_2 (d).

Table IV. Lithology interpretation for each point with its depth and thickness based on resistivity

Point	Layer	Depth (m)	Thickness (m)	Resistivity (Ωm)	Lithology
PBG_1	1	0	7.86	315.16	Tuff
	2	7.86	16.62	19.26	Sandy Tuffaceous (Aquifer)
	3	24.48	22.37	2.25	Shaley Tuff
	4	46.85	23.75	137.79	Sandy Tuffaceous (Aquifer)
	5	70.6	Inf	535.13	Tuff
PBG_2	1	0	8.09	555.67	Tuff
	2	8.09	16.36	24.99	Sandy Tuffaceous (Aquifer)
	3	24.45	33.73	6.73	Shaly Tuff
	4	58.18	32.04	110.51	Sandy Tuffaceous (Aquifer)
	5	90.22	Inf	575.87	Tuff

In the surveyed area, which falls within the Groundwater Basin (*Cekungan Air Tanah* or CAT) of Metro–Kotabumi (an inter-provincial CAT), it is suspected that the groundwater aquifer layers exist within the Tuffaceous Sand layer with varying depths and thicknesses, as detailed in Table III. Two aquifer layers have been identified at different depths: the shallow aquifer and the deep aquifer. With a relatively low groundwater potential, it is likely that water movement occurs through the inter-grain voids within these layers.

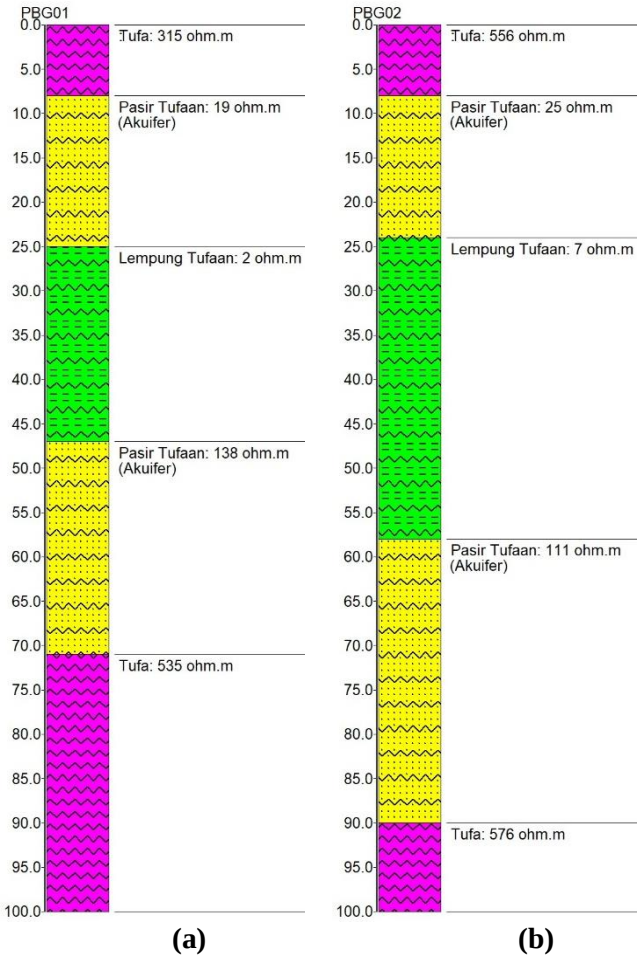

Figure 5. Subsurface lithology model for BPG_1 (a) and PBG_2 (b)

Aquifer potential within the Tuffaceous Sand layer is found at varying depths and thicknesses as indicated in Table V. The second aquifer is predicted to be a better groundwater supplier due to its thickness and its stratigraphy. The second aquifer is covered by the shaley tuff which could act like a seal and preserve the aquifer from local climate conditions such as rain.

Table V. Depth and thickness of each potential aquifer

Point	Potential Aquifer	Aquifer I	Aquifer II
PBG_1	Depth (m)	7.86 - 24.48	46.85 - 70.6
	Thickness (m)	16.62	23.75
PBG_2	Depth (m)	8.09 - 24.45	58.18 - 90.22
	Thickness (m)	16.36	32.04

4. CONCLUSIONS

From this research, it could be concluded that the subsurface layer in the study area consists of Tuff, Shaley Tuff, and Sandy Tuffaceous. Confined aquifer potential is the Tuffaceous Sand layer (2^{nd} aquifer) at 46.85 m depth for BPG_1 and 58.18 m depth for BPG_2. The thickness is 23.75 m and 32.04 m for PBG_1 and PBG_2.

References

1. W. M. Telford, L.P. Geldart, R. E. Sheriff, and D. A. Keys, **(1990)**, *Applied Geophysics*, Cambridge University Press.
2. M. H. Loke, **(2000)**, *Electrical Imaging Surveys for Environmental and Engineering Students*, Geotomo Software.
3. Y. L. Ekinci, and A. Demirci**, (2008)**, *A damped least-squares inversion program for the interpretation of Schlumberger sounding curves*, Journal of Applied Sciences 8 no. 22 4070-4078.
4. A. Akmam, and N. Y. Sudiar, **(2013)**, *Analisis Struktur Batuan dengan Metoda Inversi Smoothness-Constrained Least-Squares Data Geolistrik Konfigurasi Schlumberger di Universitas Negeri Padang Kampus Air Tawar*, Proceeding Seminar SEMIRATA FMIPA.
5. P. K. Bhattacharya, and H. P. Patra, **(1968),** *Direct Current Geoelectric Sounding: Principles and Interpretation*, Elsevier.
6. A. C. Ekwe, N. N. Onu, and K. M. Onuoha, **(2006)**, *Estimation of Aquifer Hydraulic Characteristics from Electrical Sounding Data: The Case of Middle Imo River Basin Aquifers, South- Eastern Nigeria*. Journal of Spatial Hydrology 6 no. 2 pp. 121-132.
7. J. M. Reynolds, **(1997)**, *An Introduction to Applied and Environmental Geophysics*, John Wiley & Sons.
8. G. Pratt, **(2005)**, *Applied Geophysics*, Department of Geological Sciences and Geological Engineering, Queen's University.
9. E. H. Shendi, **(2008)**, *Electrical Prospecting Methods, Applied & Environmental Geophysics.*
10. A. C. Martins, V. Elis, G. D. Tomi, J. Bettencourt, and T. Marin, **(2016)**, *Resistivity and induced polarization to support morphological modeling in limestone mining*, Geophysical international 55 no. 4 pp. 227-238.
11. E. Supriyanto, **(2007)**, *Analisis Data Geofisika: Memahami Teori Inversi, Diktat Jurusan Fisika Komputasi*, Universitas Indonesia.
12. H. Grandis, **(2009),** *Pengantar Pemodelan Inversi Geofisika*, Himpunan Ahli Geofisika Indonesia.
13. Y. L. Ekinci, Ç. Balkaya, and G. Göktürkler, **(2019)**, *Parameter estimations from gravity and magnetic anomalies due to deep-seated faults: differential evolution versus particle swarm optimization*, Turkish Journal of Earth Sciences 28 no. 6 pp. 860-881.
14. Y. Ding, W. Zhang, L. Yu, and K. Lu, **(2019)**, *The accuracy and efficiency of GA and PSO optimization schemes on estimating reaction kinetic parameters of biomass pyrolysis*, Energy 176 pp. 582-588.
15. J. L. Fernández-Martínez and E. Garcia-Gonzalo, **(2012)**, *Stochastic stability and numerical analysis of two novel algorithms of the PSO family: PP-GPSO and RR-GPSO*, International Journal on Artificial Intelligence Tools 21 no. 03 pp. 1240011.
16. A. Farduwin, R. M. Antosia, I. A. Putri, N. A. Santoso, and S. M. Irawati, **(2021)**, *Geoelectrical Data Inversion Using Particle Swarm Optimization: Case Study of Gayau Village*, Jurnal Geofisika Eksplorasi 7 no. 2 pp. 88-99.

Received: 09 Aug 2023, Accepted 13 Oct 2023